Scientia Iranica D (2019) 26(3), 1608–1616

Sharif University of Technology
Scientia Iranica
Transactions D: Computer Science & Engineering and Electrical Engineering
http://scientiairanica.sharif.edu

Solution to fractional-order Riccati differential equations using Euler wavelet method

A.T. Dincel*

Department of Mathematical Engineering, Davutpasa Campus, Yildiz Technical University, 34220, Esenler, Istanbul, Turkey.

Received 24 June 2018; received in revised form 27 September 2018; accepted 3 October 2018

KEYWORDS
Euler wavelet;
Fractional calculus;
Operational matrix;
Numerical solution;
Riccati differential equations.

Abstract. The Fractional-order Differential Equations (FDEs) have the ability to model the real-life phenomena better in a variety of applied mathematics, engineering disciplines including diffusive transport, electrical networks, electromagnetic theory, probability, and so forth. In most cases, there are no analytical solutions; therefore, a variety of numerical methods have been developed for obtaining solutions to the FDEs. In this paper, we derive numerical solutions to various fractional-order Riccati-type differential equations using the Euler Wavelet Method (EWM). The Euler wavelet operational matrix method converts the fractional differential equations to a system of algebraic equations. Illustrative examples are included to demonstrate validity and efficiency of the technique.

1. Introduction

Fractional Differential Equations (FDEs) have differentiator operators of non-integer orders. There has been an increasing interest in modeling using FDEs, since they have the ability to model the real-world phenomena more accurately in a variety of disciplines such as visco-elasticity [1], solid mechanics [2], bioengineering [3,4], economics [5], continuum mechanics [6], signal processing [7], system analysis [8], optimal control [9,10], and numerical solutions to integral and differential equations [11-13]. Since most of the fractional-order differential equations do not have analytical solutions, there have been numerous numerical methods developed to attain solutions to them, including Adomian Decomposition Method (ADM) [14,15], Variational Iteration Method (VIM) [16], Fourier transforms [17], Laplace transforms [18], eigenvector expansion [19], Homotopy Perturbation Transform Method (HPTM) [20,21], and various wavelet methods [22-25].

In many areas of engineering and applied science, such as transmission-line phenomena, optimal filtering, network synthesis, robust stabilization, image processing, control theory, etc., Riccati differential equations are utilized. Recently, various numerical methods [26-29] have been developed to solve Riccati differential equations. As for the numerical methods for fractional Riccati differential equations, Yuzbasi [30] developed a numerical method using the Bernstein polynomial; Mabood et al. [31] used the Optimal Homotopy Asymptotic Method (OHAM); Li et al. [32] applied a Reproducing Kernel Method (RKM); Odibat and Momani [33] used the Modified Homotopy Perturbation Method (MHPM); Khader [34] used the fractional Chebyshev finite difference method; and Sakar et al. [35] applied an Iterative Reproducing Kernel Hilbert Space Method (IRKHSM) to get the solutions to fractional Riccati differential equations.

In this paper, we consider the following Riccati differential equations of the form:

$$D^{\alpha}y(t)=u(t)+v(t)y(t)+w(t)[y(t)]^2,$$

*. *Tel.: +90 212 3834610*
E-mail address: artur@yildiz.edu.tr

doi: 10.24200/sci.2018.51246.2084

$$t > 0, \qquad n < \alpha \leq n+1, \tag{1}$$

which is subject to the initial conditions $y^k(0) = g_k$ and $k = 1, 2, \cdots, n-1$, where α is the fractional derivative-order parameter; n is an integer; $u(t)$, $v(t)$, and $w(t)$ are given functions; and g_k is a constant.

When α is a positive integer, the fractional equation becomes a classical Riccati differential equation.

The wavelet theory is one of the popular areas in applied science and engineering, such as segmentation, data compression, and time-frequency analysis. Wavelets generally provide accurate modeling in both time and frequency domains. Moreover, it is possible to develop fast numerical algorithms using wavelets [36]. The main advantage of using wavelet methods is that, after the discretization process, the obtained coefficient matrix of the algebraic equations is a sparse matrix, which decreases the computational load and expedites the simulation.

The focus of this paper is on solving the fractional Riccati differential equations by using Euler wavelets. The Euler wavelets are constructed by Euler polynomials. The method consists in reducing the fractional differential equation to a system of algebraic equations with unknown coefficients by using Euler wavelets. Even though the Euler polynomials are not based on orthogonal functions, they have the operational matrix of integration. In addition, numerical examples have demonstrated that the Euler wavelet performs better in approximating an arbitrary function than the Legendre and the Chebyshev wavelets do [37].

The structure of the paper is as follows: In Section 2, we present some basic definitions and properties of the fractional calculus. In Section 3, the Euler wavelets are constructed and the Euler Wavelets Operational Matrix of the Fractional Integration (EWOMFI) is derived. In Section 4, we apply EWM to the solution to the fractional Riccati differential equations through numerical examples; and the conclusion is presented in Section 5.

2. Preliminary concepts

In this section, we present definitions for the preliminary fractional calculus used in the paper.

Definition 1. The Riemann-Liouville fractional integral operator of order α is given as:

$$(I^\alpha f)(t) = \begin{cases} \frac{1}{\Gamma(\alpha)} \int\limits_0^t \frac{f(\tau)}{(t-\tau)^{1-\alpha}} d\tau & \alpha > 0, \quad t > 0, \\ f(t) & \alpha = 0 \end{cases}. \tag{2}$$

For $\alpha \geq 0$, $\beta \geq 0$, $a \geq 0$, and $\eta \geq -1$, we have the following properties of the Riemann-Liouville fractional integral:

$$\text{i)} \quad I^\alpha I^\beta = I^\beta I^\alpha, \tag{3}$$

$$\text{ii)} \quad I^\alpha (I^\beta f(t)) = I^\beta (I^\alpha f(t)) = I^{\alpha+\beta} f(t), \tag{4}$$

$$\text{iii)} \quad I^\alpha (t-a)^\eta = \frac{\Gamma(\eta+1)}{\Gamma(\alpha+\eta+1)} (t-a)^{\alpha+\eta}. \tag{5}$$

The Riemann-Liouville fractional derivative is defined by:

$$(D^\alpha f)(t) = \left(\frac{d}{dt}\right)^n (I^{n-\alpha} f)(t),$$

$$0 \leq n-1 < \alpha \leq n, \tag{6}$$

where n is an integer and $t > 0$. However, the derivative of the Riemann-Liouville operator has certain shortcomings in modeling real-world phenomena. Therefore, in this paper, we use the modified version of the fractional differential operator D^α proposed by Caputo, which is given in the following definition.

Definition 2. The Caputo definition of the fractional derivative operator is given by the following expression:

$$(D^\alpha f)(t) = \begin{cases} \frac{d^n f(t)}{dt^n} & \alpha = n \in R \\ \frac{1}{\Gamma(n-\alpha)} \int\limits_0^t \frac{f^{(n)}(\tau)}{(t-\tau)^{1-n+\alpha}} d\tau & 0 \leq n-1 < \alpha \leq n \end{cases}. \tag{7}$$

The relation between Riemann-Liouville operator and Caputo operator can be expressed by the following two common equations:

$$(D^\alpha I^\alpha f)(t) = f(t), \tag{8}$$

and:

$$(I^\alpha D^\alpha f)(t) = f(t) - \sum_{k=0}^{n-1} f^{(k)}(0^+) \frac{t^k}{k!}. \tag{9}$$

The reader is referred to [18] for more details about fractional differentiation and integration.

3. Derivation of the operational matrix of fractional integration for Euler wavelets

3.1. Wavelets and Euler wavelets

Wavelet analysis uses localized wavelike functions called 'wavelets.' A family of wavelets consists of a mother wavelet and dilated and translated versions of the mother wavelet. By making the dilation parameter a and the translation parameter b vary continuously, we can obtain the following family of continuous wavelets as [24]:

$$\psi_{a,b}(t) = |a|^{-1/2}\psi\left(\frac{t-b}{a}\right), \qquad a, b \in R, \quad a \neq 0. \tag{10}$$

If the translation and dilation parameters are chosen to have discrete values, $a = a_0^{-k}$, $b = nb_0 a_0^{-k}$, $a_0 > 1$, $b_0 > 0$, where n and k are positive integers, the family of discrete wavelets is obtained as:

$$\psi_{kn}(t) = |a_0|^{k/2}\psi(a_0^k t - nb_0). \tag{11}$$

Euler wavelets $\psi_{nm} = \psi(k, \tilde{n}, m, t)$ have 4 arguments: $\tilde{n} = n-1$, $n = 1, 2, 3, \cdots, 2^{k-1}$; k can take any positive integer value; m is the order for Euler polynomials; and t is the normalized time. Euler wavelets defined on the interval [0, 1) yield:

$$\psi_{nm}(t) = \begin{Bmatrix} 2^{\frac{k-1}{2}}\tilde{E}_m(2^{k-1}t-n+1), & \frac{n-1}{2^{k-1}} \leq t < \frac{n}{2^{k-1}} \\ 0, & \text{otherwise} \end{Bmatrix}, \tag{12}$$

and:

$$\tilde{E}_m(t) = \begin{Bmatrix} 1, & m = 0 \\ \frac{1}{\sqrt{\frac{2(-1)^{m-1}(m!)^2}{(2m)!}E_{2m+1}(0)}}, & m > 0 \end{Bmatrix}, \tag{13}$$

where $m = 0, 1, 2, \cdots, M-1$ and $n = 1, 2, 3, \cdots, 2^{k-1}$. The coefficient $\frac{1}{\sqrt{\frac{2(-1)^{m-1}(m!)^2}{(2m)!}E_{2m+1}(0)}}$ is for normality, the dilation parameter is $a = 2^{-(k-1)}$, and the translation parameter is $b = \tilde{n}2^{-(k-1)}$. $E_m(t)$ represents the Euler polynomials of the order m and given as follows [38]:

$$\sum_{k=0}^{m}\binom{m}{k}E_k(t) + E_m(t) = 2t^m, \tag{14}$$

where $\binom{m}{k}$ is the binomial coefficient. The first few Euler polynomials yield:

$$E_0(t) = 1, \qquad E_1(t) = t - \frac{1}{2}, \qquad E_2(t) = t^2 - t,$$

$$E_3(t) = t^3 - \frac{2}{3}t^2 + \frac{1}{4}, \cdots. \tag{15}$$

3.2. Function approximation

A function $f(t)$ defined over [0,1) may be expanded by Euler wavelets as:

$$f(t) = \sum_{n=1}^{2^{k-1}}\sum_{m=0}^{M-1} c_{nm}\Psi_{nm}(t) = C^T\psi(t), \tag{16}$$

where superscript T indicates transposition, and C and $\psi(t)$ are $2^{k-1} \times 1$ vectors given as:

$$C = [c_{10}, c_{11}, \cdots, c_{1(M-1)}, c_{20}, c_{21}, \cdots, c_{2(M-1)}, \\ \cdots, c_{2^{k-1}0}, c_{2^{k-1}1}, \cdots, c_{2^{k-1}(M-1)}]^T, \tag{17}$$

$$\Psi = [\Psi_{10}, \Psi_{11}, \cdots, \Psi_{1(M-1)}, \Psi_{20}, \Psi_{21}, \cdots, \Psi_{2(M-1)}, \\ \cdots, \Psi_{2^{k-1}0}, \Psi_{2^{k-1}1}, \cdots, \Psi_{2^{k-1}(M-1)}]^T. \tag{18}$$

Now, let us define $m' = 2^{k-1}M$. The Euler wavelet matrix is defined as:

$$\phi_{m' \times m'} = \left[\Psi(t_1), \Psi(t_2), \Psi(t_3), \cdots, \Psi(t_{m'})\right], \tag{19}$$

where t_i represents collocation points. If the collocation points are chosen as $t_i = \frac{i-0.5}{m'}$, $i = 1, 2, 3, \cdots, m'$, the Euler wavelet matrix for $k = 2$, $M = 3$, and $\alpha = 0.5$ becomes:

$$\phi_{m' \times m'}(t) = \begin{bmatrix} 1.4142 & 1.4142 & 1.4142 & 0 & 0 & 0 \\ -0.2357 & 0 & 0.2357 & 0 & 0 & 0 \\ -0.0802 & -0.1443 & -0.0802 & 0 & 0 & 0 \\ 0 & 0 & 0 & 1.4142 & 1.4142 & 1.4142 \\ 0 & 0 & 0 & -0.2357 & 0 & 0.2357 \\ 0 & 0 & 0 & -0.0802 & -0.1443 & -0.0802 \end{bmatrix}. \tag{20}$$

3.3. Euler wavelet operational matrix of fractional integration

3.3.1. Block pulse functions

An m' set of Block Pulse Functions (BPFs) is defined as:

$$b_i(t) = \begin{Bmatrix} 1 & (i-1)/m' \leq t < i/m' \\ 0 & \text{otherwise} \end{Bmatrix}, \tag{21}$$

where $i = 1, 2, 3, \cdots, m'$. The function $b_i(t)$ is disjoint and orthogonal. For $t \in [0, 1)$:

$$b_i(t)b_j(t) = \begin{Bmatrix} 0 & i \neq j \\ b_i(t) & i = j \end{Bmatrix}, \tag{22}$$

$$\int_0^1 b_i(\tau)b_j(\tau)d\tau = \begin{Bmatrix} 0 & i \neq j \\ 1/m' & i = j \end{Bmatrix}. \tag{23}$$

It is known that any square integral function $f(t)$

defined in [0,1) can be expanded into an m' set of BPFs as:

$$f(t)=\sum_{i=1}^{m'} f_i b_i(t)=f^T B_{m'}(t), \tag{24}$$

where:

$$f=[f_1,f_2,\cdots,f_{m'}]^T,$$

$$B_{m'}(t)=[b_1(t),b_2(t),\cdots,b_{m'}(t)]^T,$$

and f_i is given as:

$$f_i=\frac{1}{m'}\int_{(i-1)/m'}^{i/m'} f(t)b_i(t)dt. \tag{25}$$

The Euler wavelet matrix can also be expanded to an m' set of BPFs as:

$$\psi(t)=\phi_{m'\times m'}B_{m'}(t). \tag{26}$$

The block pulse operational matrix for fractional integration F^α is defined as [39]:

$$\left(I^\alpha B_{m'}\right)(t)\approx F^\alpha B_{m'}(t), \tag{27}$$

where:

$$F^\alpha=\frac{1}{m^\alpha}\frac{1}{\Gamma(\alpha+2)}\begin{bmatrix}1 & \xi_1 & \xi_2 & \xi_3 & \cdots & \xi_{m'-1}\\ 0 & 1 & \xi_1 & \xi_2 & \cdots & \xi_{m'-2}\\ 0 & 0 & 1 & \xi_1 & \cdots & \xi_{m'-3}\\ \vdots & \vdots & \ddots & \ddots & \vdots & \vdots\\ 0 & 0 & \cdots & 0 & 1 & \xi_1\\ 0 & 0 & \cdots & 0 & 0 & 1\end{bmatrix}, \tag{28}$$

with $\xi_k=(k+1)^{\alpha+1}-2k^{\alpha+1}+(k-1)^{\alpha+1}$.

Now, let us derive the Euler Wavelet Operational Matrix of Fractional Integration (EWOMFI):

$$(I^\alpha\psi)(t)\approx P^\alpha_{m'\times m'}\psi(t), \tag{29}$$

where matrix $P^\alpha_{m'\times m'}$ is called the EWOMFI.

Using Eqs. (26) and (27), we obtain:

$$\begin{aligned}(I^\alpha\Psi)(t)&\approx(I^\alpha\phi_{m'\times m'}B_{m'})(t)\\ &=\phi_{m'\times m'}(I^\alpha B_{m'})(t)\approx\phi_{m'\times m'}F^\alpha B_{m'}(t).\end{aligned} \tag{30}$$

Furthermore, using Eqs. (26), (29), and (30) yields:

$$\begin{aligned}P^\alpha_{m'\times m'}\Psi(t)&\approx(I^\alpha\Psi)(t)\approx\phi_{m'\times m'}F^\alpha B_{m'}(t)\\ &=\phi_{m'\times m'}F^\alpha\phi^{-1}_{m'\times m'}\Psi(t).\end{aligned}$$

The resulting EWOMFI $P^\alpha_{m'\times m'}$ becomes:

$$P^\alpha_{m'\times m'}\approx\phi_{m'\times m'}F^\alpha\phi^{-1}_{m'\times m'}. \tag{31}$$

As an example, the EWOMFI for $k=2$, $M=3$, and $\alpha=0.5$ yields:

$$P^\alpha_{m'\times m'}=\begin{bmatrix}0.4616 & 1.2601 & -0.9787 & 0.5012 & -0.6034 & 0.8425\\ 0.0219 & 0.2243 & 0.6305 & 0.0179 & -0.0449 & 0.0940\\ -0.0217 & -0.1061 & 0.2354 & -0.0352 & 0.0410 & -0.0545\\ 0 & 0 & 0 & 0.4616 & 1.2601 & -0.9787\\ 0 & 0 & 0 & 0.0219 & 0.2243 & 0.6305\\ 0 & 0 & 0 & -0.0217 & -0.1061 & 0.2354\end{bmatrix}. \tag{32}$$

We use $A\otimes B=(a_{ij}\times b_{ij})_{m'\times m'}$ for the multiplication of two matrices of size $m'\times m'$.

The reader is referred to [37] for the convergence analysis of the Euler wavelet basis.

4. Numerical examples

In this section, we provide three numerical examples to demonstrate the accuracy of the Euler Wavelet Method (EWM). Matlab R2017a has been used for the simulations. We have also calculated the order of convergence, which is expressed as [40,41]:

$$\text{converg. rate}=\frac{\log\left(\frac{\text{solution}(i-1)-\text{solution}(i-2)}{\text{solution}(i-2)-\text{solution}(i-3)}\right)}{\log(2)}. \tag{33}$$

4.1. Example 1

$$D^\alpha y(t)+y(t)-y^2(t)=0, \tag{34}$$

with initial condition $y(0)=1/2$, where the parameter α denotes the fractional time derivative with $0<\alpha\leq 1$. The exact solution for $\alpha=1$ is given as $y(t)=\frac{e^{-t}}{1+e^{-t}}$. Let:

$$D^\alpha y(t)\approx C^T\psi(t). \tag{35}$$

Then, with the initial conditions, we have:

$$y(t)\approx(I^\alpha D^\alpha y)(t)\approx C^T P^\alpha_{m'\times m'}\psi(t)+y(0). \tag{36}$$

Substituting Eq. (26) into Eq. (36) the following is obtained:

$$\begin{aligned}y(t)\approx&C^T P^\alpha_{m'\times m'}\phi_{m'\times m'}B_{m'}(t)\\ &+\left[\frac{1}{2},\frac{1}{2},\cdots,\frac{1}{2}\right]B_{m'}(t).\end{aligned} \tag{37}$$

Let:

$$C^T P^{\alpha}_{m'\times m'}\phi_{m'\times m'} = [a_1, a_2, \cdots, a_{m'}], \tag{38}$$

using Eq. (26), we have:

$$[y(t)]^2 = [a_1^2, a_2^2, \cdots, a_{m'}^2]B_{m'}(t) + 2KB_{m'}(t) + \left[\frac{1}{4}, \frac{1}{4}, \cdots \frac{1}{4}\right] B_{m'}(t), \tag{39}$$

where:

$$K = C^T P^{\alpha}_{m'\times m'}\phi_{m'\times m'} \otimes \left[\frac{1}{2}, \frac{1}{2}, \cdots, \frac{1}{2}\right]. \tag{40}$$

Substituting Eqs. (39), (37), and (35) into Eq. (34), we get:

$$C^T\phi_{m'\times m'} + C^T P^{\alpha}_{m'\times m'}\phi_{m'\times m'} + \left[\frac{1}{2}, \frac{1}{2}, \cdots, \frac{1}{2}\right] - [a_1^2, a_2^2, \cdots, a_{m'}^2] - 2K - \left[\frac{1}{4}, \frac{1}{4}, \cdots, \frac{1}{4}\right] = 0. \tag{41}$$

This nonlinear system of equations can be solved using Newton iteration method and the vector of unknown coefficients C can be computed. After calculating the vector C, we can obtain the numerical solution for $y(t)$ using Eq. (36). Figure 1 shows the EWM solution for $m' = 80$ and the exact solution for $\alpha = 1$. The comparison between the exact solution and EWM solution for various values of m' is presented in Table 1. As can be seen in the table, even fairly small values of $k = 3$ and $M = 3$ ($m' = 12$) produce a good approximation. As m' increases, the absolute error decreases to the order of E-9. EWM solution for $m' = 80$ with various fractional values of α is given in Figure 2. As α approaches 1, the solution to the fractional-order differential equation approaches the solution to integer-order differential equation. The order of convergence is given in Table 2. As it is shown [41,42], this rate tends to 2.

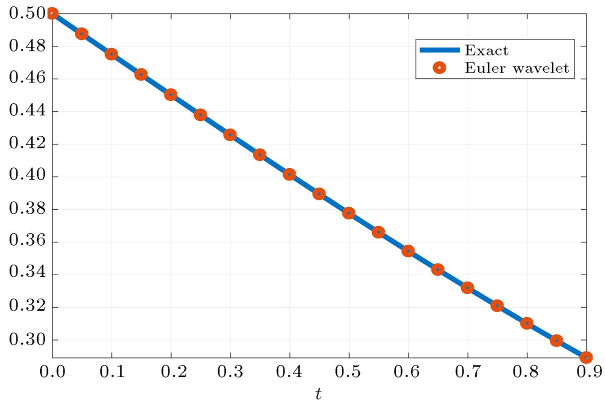

Figure 1. The solution of EWM for $\alpha = 1$ and the exact solution for Example 1.

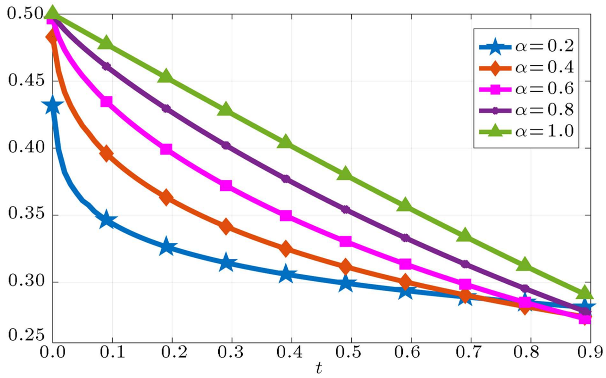

Figure 2. The solution of EWM for various values of α for Example 1.

4.2. Example 2

Consider the following Riccati differential equation:

$$D^{\alpha}y(t) - 2y(t) + y^2(t) - 1 = 0.$$

$$y(0) = 0, \tag{42}$$

where $0 < \alpha \leq 1$. The exact solution for $\alpha = 1$ is given as:

Table 1. Comparison of the exact solution and EWM with $\alpha = 1$ and various values of m' for Example 1.

t	Exact solution	$m' = 12$	$m' = 24$	$m' = 48$	$m' = 96$	$m' = 192$	$m' = 384$
0.0	0.5000000	0.5000223	0.5000028	0.5000004	0.5000000	0.5000000	0.5000000
0.1	0.4750208	0.4750248	0.4750229	0.4750213	0.4750209	0.4750208	0.4750208
0.2	0.4501660	0.4501822	0.4501699	0.4501669	0.4501662	0.4501661	0.4501660
0.3	0.4255575	0.4255764	0.4255623	0.4255588	0.4255578	0.4255576	0.4255575
0.4	0.4013123	0.4013419	0.4013188	0.4013140	0.4013128	0.4013124	0.4013124
0.5	0.3775407	0.3775881	0.3775507	0.3775429	0.3775412	0.3775408	0.3775407
0.6	0.3543437	0.3543778	0.3543529	0.3543460	0.3543443	0.3543438	0.3543437
0.7	0.3318122	0.3318532	0.3318224	0.3318147	0.3318128	0.3318124	0.3318123
0.8	0.3100255	0.3100667	0.3100358	0.3100282	0.3100262	0.3100257	0.3100256
0.9	0.2890505	0.2890953	0.2890613	0.2890532	0.2890512	0.2890507	0.2890505

Table 2. The solution and convergence rate at point $t = 0.5$ for Example 1.

i	m'	Solution (i)	Convergence rate
1	12	0.3775881	—
2	24	0.3775507	—
3	48	0.3775429	2.2615
4	96	0.3775412	2.1979
5	192	0.3775408	2.0874
6	384	0.3775407	2.0000

$$y(t) = 1 + \sqrt{2}\tanh\left(\sqrt{2}t + \frac{1}{2}\log\left(\frac{\sqrt{2}-1}{\sqrt{2}+1}\right)\right).$$

Using the same approximation as that given for Example 1 in detail, we obtain the following nonlinear equation, the solution to which produces C coefficients:

$$C^T\phi_{m'\times m'} - 2C^T P^{\alpha}_{m'\times m'}\phi_{m'\times m'} + [a_1^2, a_2^2, \cdots, a_{m'}^2] - [1, 1, \cdots, 1] = 0. \tag{43}$$

where $[a_1, a_2, \cdots, a_{m'}] = C^T P^{\alpha}_{m'\times m'}\phi_{m'\times m'}$. After finding the coefficient vector C, we can again obtain the numerical solution for $y(t)$ using Eq. (36). Figure 3 shows the solution of EWM for $m' = 80$ and the exact solution for $\alpha = 1$. The comparison between absolute errors of the EWM solution and some other solution methods for the fractional differential equation with various values of m' is presented in Table 3. The results indicate two important features; firstly, unlike in the other methods, the absolute error does not increase in the EWM as t increases and secondly, for the m' values greater than 96, the EWM provides better approximation. Another comparison for $\alpha = 0.75$ is given with various values of m' in Table 4. Euler wavelet solution for $m' = 80$ with various fractional values of α is given in Figure 4. Again, it can be stated that the solution to the fractional-order differential equation approaches the solution to integer-order differential equation as α approaches 1.

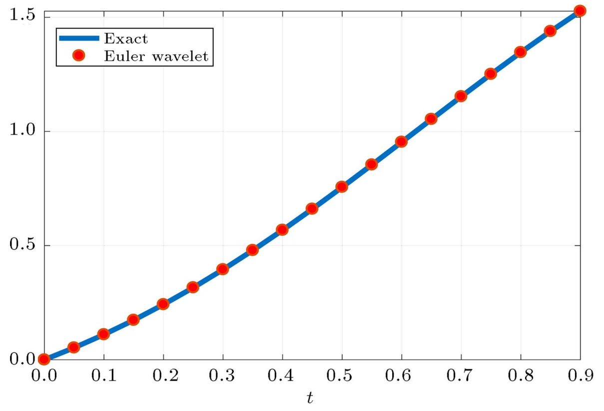

Figure 3. The solution of EWM for $\alpha = 1$ and the exact solution for Example 2.

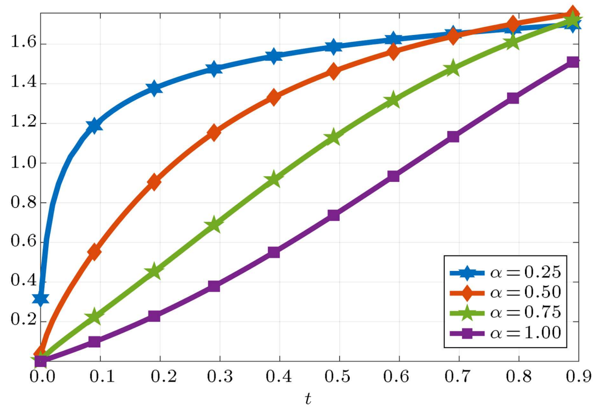

Figure 4. The solution of EWM for various values of α for Example 2.

4.3. Example 3

Consider the following Riccati differential equation:

$$D^{\alpha}y(t) + y^2(t) - 1 = 0,$$

$$y(0) = 0, \tag{44}$$

where $0 < \alpha \leq 1$. The exact solution for $\alpha = 1$ is given as $y(t) = \frac{e^{2t}-1}{e^{2t}+1}$.

Table 3. The absolute errors of EWM and some other solution methods for the fractional-order differential equation with $\alpha = 1$ and various values of m' for Example 2.

t	$m' = 24$	$m' = 48$	$m' = 96$	$m' = 192$	$m' = 384$	MHPM [33]	IRKHSM [27]	OHAM [31]
0.1	5.52E-04	1.38E-04	3.43E-05	8.57E-06	2.14E-06	1.00E-06	3.58E-05	3.20E-05
0.2	6.47E-04	1.63E-04	4.06E-05	1.01E-05	2.54E-06	1.20E-05	7.58E-05	2.90E-05
0.3	7.27E-04	1.78E-04	4.46E-05	1.12E-05	2.80E-06	1.00E-06	1.20E-04	1.10E-03
0.4	7.44E-04	1.85E-04	4.56E-05	1.14E-05	2.86E-06	3.03E-04	1.66E-04	2.50E-03
0.5	5.20E-04	1.52E-04	4.07E-05	1.05E-05	2.66E-06	1.55E-03	2.12E-04	4.40E-03
0.6	5.84E-04	1.47E-04	3.78E-05	9.44E-06	2.34E-06	4.69E-03	2.52E-04	5.50E-03
0.7	4.56E-04	1.22E-04	3.05E-05	7.49E-06	1.87E-06	1.05E-02	2.87E-04	5.50E-03
0.8	3.79E-04	8.82E-05	2.22E-05	5.64E-06	1.41E-06	1.89E-02	3.40E-04	3.80E-03
0.9	2.66E-04	6.63E-05	1.60E-05	4.02E-06	1.01E-06	2.80E-02	4.90E-04	3.40E-03

Table 4. Comparison of the EWM and some other solution methods for the fractional-order differential equation with $\alpha = 0.75$ for Example 2.

t	$m' = 24$	$m' = 48$	$m' = 96$	$m' = 192$	$m' = 384$	RKM [32]	MHPM [33]	IRKHSM [35]
0.2	0.476341	0.475422	0.475178	0.475117	0.475117	0.4695	0.4288	0.4730
0.4	0.939340	0.938740	0.938586	0.938548	0.938548	0.9335	0.8914	0.9368
0.5	1.149579	1.149198	1.149097	1.149070	1.149070	1.1448	1.1327	1.1475
0.6	1.334765	1.334444	1.334360	1.334339	1.334339	1.3309	1.3702	1.3330
0.8	1.623300	1.623073	1.623011	1.622995	1.622995	1.6215	1.7948	1.6220

The nonlinear equation used to obtain the coefficient vector C becomes:

$$C^T \phi_{m' \times m'} - [1, 1, \cdots, 1] + [a_1^2, a_2^2, \cdots, a_{m'}^2] = 0, \tag{45}$$

where $[a_1, a_2, \cdots, a_{m'}] = C^T P^{\alpha}_{m' \times m'} \phi_{m' \times m'}$. As in the other two examples, the coefficient vector C is used to obtain the numerical solution for $y(t)$ using Eq. (36). Figure 5 presents the solution of EWM for $m' = 80$ and the exact solution for $\alpha = 1$. The comparison between absolute errors of the Euler wavelet solution and some other solution methods for the fractional differential equation with $m' = 384$ is provided in Table 5. As can be seen in the table, EWM provides better approximation. Another comparison of the numerical results with $\alpha = 0.75$ is given for various values of m' in Table 6.

Euler wavelet solution with $m' = 80$ for various fractional values of α is given in Figure 6. Again, the results show that the solution to the fractional-order differential equation approaches the solution to integer-order differential equation as α approaches 1.

5. Conclusion

In this paper, numerical solutions to various fractional-order Riccati-type differential equations were obtained using the Euler Wavelet Method (EWM). The operational matrix of fractional integration was obtained for Euler wavelets and applied for obtaining the solution to several fractional-order Riccati differential equations. It has been shown elsewhere that the Euler wavelets perform better than other wavelet methods [37].

The Euler Wavelet Method (EWM) results in sparse coefficient matrices; therefore, it has shorter simulation duration and lower memory requirements. The numerical solutions given in detail in Section 4 proved that the EWM was a better approximation to the exact solution than other numerical solution methods when larger values of m' were used for integer orders (corresponding to taking more samples for dis-

Table 5. The absolute errors of EWM and some other solution methods for the fractional-order differential equation with $\alpha = 1$ for Example 3.

t	EWM	VIM [28]	MHPM [33]	IRKHSM [27]
0.1	1.117589E-07	5.00E-11	0	9.05E-06
0.2	2.100616E-07	4.39E-09	0	1.72E-05
0.3	2.822560E-07	1.56E-07	1.00E-06	2.38E-05
0.4	3.281852E-07	1.97E-06	5.00E-06	2.85E-05
0.5	3.464860E-07	1.38E-05	3.90E-05	3.11E-05
0.6	3.307795E-07	6.61E-05	1.93E-04	3.17E-05
0.7	2.962782E-07	2.43E-04	7.37E-04	3.07E-05
0.8	2.480617E-07	7.35E-04	2.33E-03	2.81E-05
0.9	1.922805E-07	1.91E-03	6.37E-03	2.32E-05

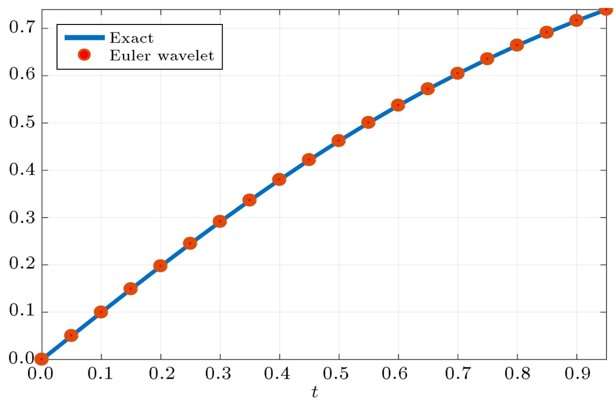

Figure 5. The solution of EWM for $\alpha = 1$ and the exact solution for Example 3.

Table 6. Comparison of the EWM and some other solution methods for the fractional-order differential equation with $\alpha = 0.75$ for Example 3.

t	$m' = 24$	$m' = 48$	$m' = 96$	$m' = 192$	$m' = 384$	RKM [32]	Method in [30]	MHPM [33]	IRKHSM [35]
0.2	0.309815	0.309924	0.309962	0.309972	0.309972	0.3073	0.3099	0.3138	0.3100
0.4	0.481539	0.481609	0.488162	0.481630	0.481630	0.4803	0.4816	0.4929	0.4816
0.6	0.5977565	0.597762	0.597780	0.597782	0.597782	0.5975	0.5977	0.5974	0.5978
0.8	0.6788444	0.678850	0.6788495	0.678850	0.678850	0.6796	0.6788	0.6604	0.6788

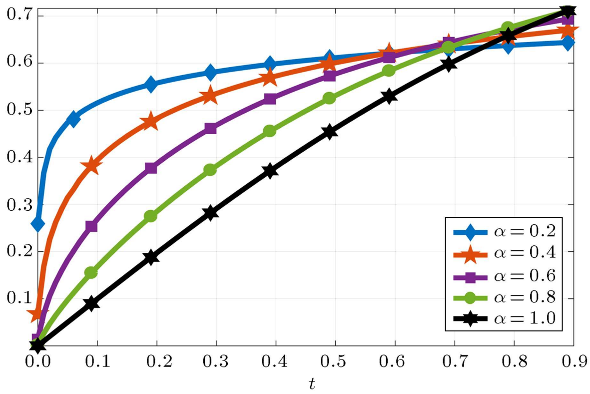

Figure 6. The solution of EWM for various values of α for Example 3.

cretization). Moreover, the numerical solutions for the fractional orders showed that as α approached 1, they approached those for the integer orders. The results proved that the method could be applicable to various other fractional differential equations.

The approach used here can be applied to the related differential equations in [43].

References

1. Colinas-Armijo, N., Di Paola, M., and Pinnola, F.P. "Fractional characteristic times and dissipated energy in fractional linear viscoelasticity", *Commun. Nonlinear Sci. Numer. Simul.*, **37**, pp. 14-30 (2016).
2. Rossikhin, Y.A. and Shitikova M.V. "Application of fractional calculus for dynamic problems of solid mechanics: novel trends and recent results", *Appl. Mech. Rev.*, **63**(1), pp. 1-52 (2009).
3. Magin, R.L. and Ovadia M. "Modeling the cardiac tissue electrode interface using fractional calculus", *J. Vib. Control*, **14**(9-10), pp. 1431-1442 (2008).
4. Sommacal, L., Melchior, P., Oustaloup, A., Cabelguen, J.M., and Ijspeert, A.J. "Fractional multi-models of the frog gastrocnemius muscle", *J. Vib. Control*, **14**(9-10), pp. 1415-1430 (2008).
5. Baillie, R.T. "Long memory processes and fractional integration in econometrics", *J. Econom.*, **73**(1), pp. 5-59 (1996).
6. Carpinteri, A. and Mainardi, F., *Fractals and Fractional Calculus in Continuum Mechanics*, Springer-Verlag, Vien, New York (1997).
7. Lima, M.F.M., Machado, J.A.T., and Crisóstomo, M. "Experimental signal analysis of robot impacts in a fractional calculus perspective", *J. Adv. Comput. Intell. Intell. Inform.*, **11**, pp. 1079-1085 (2007).
8. Chen, C. and Hsiao, C. "Haar wavelet method for solving lumped and distributed-parameter systems", *IEE P-Contr. Theor. Appl.*, **144**(1), pp. 87-94 (1997).
9. Karimi, H., Moshiri, B., Lohmann, B., and Maralani, P. "Haar wavelet-based approach for optimal control of second-order linear systems in time domain", *J. Dyn. Control Syst.*, **11**(2), pp. 237-252 (2005).
10. Sadek, I., Abualrub, T., and Abukhaled, M. "A computational method for solving optimal control of a system of parallel beams using Legendre wavelets", *Math. Comput. Model*, **45**(9-10), pp. 1253-1264 (2007).
11. Babolian, E., Masouri, Z., and Hatamzadeh-Varmazyar, S. "Numerical solution of nonlinear Volterra-Fredholm integro-differential equations via direct method using triangular functions", *Comput. Math. Appl.*, **58**(2), pp. 239-247 (2009).
12. Kajani, M. and Vencheh, A. "The Chebyshev wavelets operational matrix of integration and product operation matrix", *Int J. Comput. Math.*, **86**(7), pp. 1118-1125 (2008).
13. Razzaghi, M. and Yousefi, S. "The Legendre wavelets operational matrix of integration", *Int. J. Syst. Sci.*, **32**(4), pp. 495-502 (2001).
14. El-Wakil, S.A., Elhanbaly, A., and Abdou, M.A. "Adomian decomposition method for solving fractional nonlinear differential equations", *Appl. Math. Comput.*, **182**(1), pp. 313-324 (2006).
15. Momani, S. and Odibat, Z. "Numerical approach to differential equations of fractional order", *J. Comput. Appl. Math.*, **207**(1), pp. 96-110 (2007).
16. Das, S. "Analytical solution of a fractional diffusion equation by variational iteration method", *Comput. Math. Appl.*, **57**(3), pp. 483-487 (2009).
17. Gaul, L., Klein, P., and Kemple, S. "Damping description involving fractional operators", *Mech. Syst. Signal Pr.*, **5**(2), pp. 81-88 (1991).
18. Podlubny, I., *Fractional Differential Equations: An Introduction to Fractional Derivatives, Fractional Differential Equations, to Methods of Their Solution and Some of their Applications*, New York, Academic Press (1999).
19. Suarez, L. and Shokooh, A. "An eigenvector expansion method for the solution of motion containing fractional derivatives", *J. Appl. Mech.*, **64**(3), pp. 629-635 (1997).
20. Kumar, S. "A new fractional analytical approach for treatment of a system of physical models using Laplace transform", *Sci. Iran. B*, **21**(5), pp.1693-1699 (2014).
21. Khader, M.M. "Application of homotopy perturbation method for solving nonlinear fractional heat-like equations using Sumudu transform", *Sci. Iran. B*, **24**(2), pp. 648-655 (2017).
22. Xu, X. and Xu, D. "Legendre wavelets method for approximate solution of fractional-order differential equations under multi-point boundary conditions", *Int. J. Comput. Math.*, **95**(5), pp. 998-1014 (2018).
23. Wang, Y.X. and Fan, Q.B. "The second kind Chebyshev wavelet method for solving fractional differential equation", *Appl. Math. Comput.*, **218**(17), pp. 8592-8601 (2012).

24. Shah, F.A. and Abass, R. "Haar wavelet operational matrix method for the numerical solution of fractional order differential equations", *Nonlinear Engin.*, **4**(4), pp. 203-213 (2015).
25. Rahimkhani, P., Ordokhani, Y., and Babolian, E. "Numerical solution of fractional pantograph differential equations by using generalized fractional-order Bernoulli wavelet", *J. Comput. Appl. Math.*, **309**(1), pp. 493-510 (2017).
26. El-Tawil, M.A., Bahnasawi, A.A., and Abdel-Naby, A. "Solving Riccati differential equation using Adomian's decomposition method", *Appl. Math. Comput.*, **157**(2), pp. 503-514 (2004).
27. Sakar M. "Iterative reproducing kernel Hilbertspaces method for Riccati differential equations", *J. Comput. Appl. Math.*, **309**, pp. 163-174 (2017).
28. Batiha, B., Noorani, M.S.M., and Hashim, I. "Application of variational iteration method to general Riccati equation", *Int. Math. Forum*, **2**(56), pp. 2759-2770 (2007).
29. Geng, F., Lin, Y., and Cui, M. "A piecewise variational iteration method for Riccati differential equations", *Comput. Math. Appl.*, **58**(11-12), pp. 2518-2522 (2009).
30. Yuzbası, S. "Numerical solutions of fractional Riccati type differential equations by means of the Bernstein polynomials", *Appl. Math. Comput.*, **219**(11), pp. 6328-6343 (2013).
31. Mabood, F., Ismail, A.I., and Hashim, I. "Application of optimal homotopy asymptotic method for the approximate solution of Riccati equation", *Sains Malays.*, **42**(6), pp. 863-867 (2013b).
32. Li, X.Y., Wu, B.Y., and Wang, R.T. "Reproducing kernel method for fractional Riccati differential equations", *Abstr. Appl. Anal.*, Article ID 970967, 6 pages (2014).
33. Odibat, Z. and Momani, S. "Modified homotopy perturbation method: application to quadratic Riccati differential equation of fractional order", *Chaos Solitons Fractals*, **36**(1), pp. 167-174 (2008).
34. Khader, M.M. "Numerical treatment for solving fractional Riccati differential equation", *J. Egyptian Math. Soc.*, **21**(1), pp. 32-37 (2013).
35. Sakar, M.G., Akgül, A., and Baleanu, D. "On solutions of fractional Riccati differential equations", *Adv. Differ. Equ.*, **39**, pp. 1-10 (2017).
36. Beylkin, G., Coifman, R., and Rokhlin, V. "Fast wavelet transforms and numerical algorithms", *I. Commun. Pure Appl. Math.*, **44**(2), pp. 141-183 (1991).
37. Wang, Y. and Zhu, L. "Solving nonlinear Volterra integro-differential equations of fractional order by using Euler wavelet method", *Adv. Differ. Equ.*, **27**, pp. 1-16 (2017).
38. He, Y. and Wang, C. "Recurrence formulae for Apostol-Bernoulli and Apostol-Euler polynomials", *Adv. Differ. Equ.*, **209**, pp. 1-16 (2012).
39. Kilicman, A. "Kronecker operational matrices for fractional calculus and some applications", *Appl. Math. Comput.*, **187**(1), pp. 250-265 (2007).
40. Atkinson, K.E., *An Introduction to Numerical Analysis*, Wiley, New York (1978).
41. Majak, J., Shvartsman, B., Karjust, K., Mikola, M., Haavaj oe, A., and Pohlak, M. "On the accuracy of the Haar wavelet discretization method", *Compos. Part B*, **80**, pp. 321-327 (2015).
42. Majak, J., Pohlak, M., Karjust, K., Eerme, M., Kurnitski, J., and Shvartsman, B.S. "New higher order Haar wavelet method: Application to FGM structures", *Compos. Struct.*, **201**, pp. 71-78 (2018).
43. Tural Polat S.N. "The vector-matrix form numerical simulations for time-derivative cellular neural networks", *Int. J. Numer. Model.*, **31**(5), pp. 1-13 (2018).

Biography

Arzu Turan Dincel received the PhD degree in Mathematical Engineering from the Yildiz Technical University, Istanbul, Turkey. She is currently an Assistant Professor in the Mathematical Engineering Department of Yildiz Technical University. Some of her research interests include fractional calculus, fracture mechanics, and finite element method.